High-resolution LEED profile analysis and diffusion barrier estimation for submonolayer homoepitaxy of Ag/Ag(100)

L. Bardotti,* C. R. Stoldt, C. J. Jenks, M. C. Bartelt,† J. W. Evans, and P. A. Thiel
Departments of Chemistry and Mathematics, IPRT, and Ames Laboratory, Iowa State University, Ames, Iowa 50011
(Received 16 December 1997)

We present a high-resolution low-energy electron diffraction study of two-dimensional island distributions formed by depositing 0.3 ML of Ag on Ag(100). The substrate temperature ranged between 170 and 295 K. From the ring structure or ''splitting'' of the diffraction profiles, we determine the behavior of the spatial correlation length characterizing the island distribution. The precise relationship between this correlation length and the mean island separation is also determined via an analysis of kinematic diffraction from island distributions in a realistic model of nucleation and growth. Resulting estimates of this separation are consistent with those based on results from a previous scanning tunneling microscopy study at 295 K. From the Arrhenius behavior of the correlation length, we estimate a terrace diffusion barrier for Ag on Ag(100) of 0.40 ± 0.04 eV, with a vibrational prefactor of about 3×10^{13} s^{-1}. [S0163-1829(98)08819-5]

I. INTRODUCTION

High-resolution surface-sensitive diffraction techniques provide a powerful tool for analysis of submonolayer and multilayer thin-film structure.[1] The utility of these techniques is enhanced if the kinematic or single-scattering approximation can be applied to analyze the shape of the diffuse intensity profile (i.e., the variation of diffuse intensity with lateral momentum transfer). This approximation ensures a simple and direct Fourier transform relationship between the diffracted intensity and certain spatial-pair correlation functions describing surface structure.[2–4] The kinematic approximation is generally assumed valid for analysis of the shape of high-resolution low-energy electron diffraction (HRLEED) profiles, but not for the variation of intensity with energy.[3] Here we present experimental data, together with a theoretical analysis, for HRLEED profiles for homoepitaxy of Ag on Ag(100) in the submonolayer regime, where the overlayer can be best described as a distribution of two-dimensional near-square islands.[5]

General aspects of the relationship between the shape of the diffraction profile and submonolayer film structure are well recognized. For randomly distributed islands, the diffraction profile is simply a weighted sum of intensities from individual islands, and thus is determined by the island shape and size distribution.[4] For distributions with a depleted population of nearby island pairs, a well-defined characteristic length L_c emerges that reflects the average island separation $L_{\rm av}$. This produces a corresponding ring structure to the diffuse intensity, and thus a ''splitting'' of the diffraction profile.[6] Such splitting was first observed and discussed in an experimental study of submonolayer W/W(110) deposition by Hahn, Clabes, and Henzler.[7] A variety of simple, typically one-dimensional models for the adlayer statistics (e.g., specifying island size and separation distributions) have further clarified these ideas.[6] However, a precise quantitative analysis of diffraction profiles must be based upon an accurate description of the nontrivial spatial correlations characterizing the two-dimensional island distribution. Such a description is provided by Monte Carlo simulations of realistic models for nucleation and growth of islands during deposition.[8] These quantify the depletion of nearby pairs of islands, intrinsic to the nucleation process,[9] as well as the associated profile splitting.[8]

Scanning tunneling microscopy (STM) provides the possibility of direct access to real-space information about the island distribution. Thus, it is natural to compare such direct observations against predictions from the type of analysis described above of reciprocal-space HRLEED data. However, to date, such careful comparisons are lacking, even for the simple metal(100) homoepitaxial systems of interest here.[5,10–15] Thus, we are motivated to provide such a comparison for the Ag/Ag(100) system, exploiting our previous STM study,[5] and focusing on the mean-island separation $L_{\rm av}$.

A traditional goal of analyzing the behavior of the mean-island separation $L_{\rm av}$, or density $N_{\rm av}=(L_{\rm av})^{-2}$, in nucleation and growth processes, is the estimation of the barrier for terrace diffusion E_d.[9] Clearly, both HRLEED and STM techniques are well suited to this task. Apart from field ion microscopy studies for a specific subset of metal-on-metal systems,[16] there is actually only a limited set of reliable data on such barriers. Thus, these results are of considerable interest both in their own right, and for comparison with theoretical estimates from various electronic structure calculations. Thus, a key application of our HRLEED analysis is the estimation of E_d for the Ag/Ag(100) system.

In Sec. II, we describe the experimental setup and procedure for our HRLEED analysis of the Ag/Ag(100) system. We also comment briefly on the procedure and results of our previous STM study. A summary of the relevant aspects of kinematic diffraction theory is presented in Sec. III, together with some results relating diffraction profile splitting to the mean island separation. The key HRLEED results of this study are described in Sec. IV. Discussion of these results, and detailed comparison with the previous STM results, is presented in Sec. V. A summary is provided in Sec. VI.

II. THE Ag/Ag(100) SYSTEM AND EXPERIMENTAL TECHNIQUES

First, it is appropriate to note that the submonolayer Ag/Ag(100) system has been studied previously by several

diffraction techniques: LEED,[13,14] He-beam scattering,[14] and surface x-ray scattering.[15] While all these studies reported the expected splitting of the diffraction profiles, none have quantified the behavior of $L_{\rm av}$ or extracted estimates of E_d. Thus, the full potential of these techniques has not been exploited.

Our experiments were performed in an ultrahigh vacuum chamber with a base pressure of 6×10^{-11} to 2×10^{-10} Torr, equipped with both an Omicron HRLEED system, and an Omicron room-temperature STM. Silver was deposited on an Ag(100) crystal from a resistively heated liquid-nitrogen-shrouded source. In the HRLEED studies with the substrate held at room temperature, a high-quality Ag crystal with typical terrace widths of 1000 Å was used. HRLEED studies were also performed for lower substrate temperatures down to 170 K, using a lower-quality crystal with typical terrace widths of 600 Å. In both cases, terrace widths are far larger than the mean island separation, so the influence of steps or of finite terraces should be small. HRLEED intensities were obtained near an out-of-phase condition for destructive interference between scattering from successive layers for the Ag/Ag(100) system. At the (0,0) beam corresponding to zero lateral momentum transfer, the out-of-phase condition corresponds to $q_z b=(2n+1)\pi$, for integer n. Here, q_z is the vertical momentum transfer, and b is the interlayer spacing. We choose an energy of 110.4 eV, corresponding to $n=3$, which is consistent with the known value of $b=2.05$ Å for the fcc Ag crystal. All the profiles shown are taken in the $\langle 110\rangle$ direction, and were measured within about 2.5–5 min following deposition. The deposition source was calibrated by monitoring the Bragg intensity oscillations near the out-of-phase condition, during deposition of a few monolayers of Ag. The minima (maxima) correspond to half (full) monolayer coverages. All of the diffraction profiles shown below were taken after deposition of 0.3 ML of Ag, and for similar deposition fluxes in the range of $2-4\times10^{-3}$ ML/s.

As noted in the Introduction, we will compare the results from analysis of the HRLEED profiles with those from our previous STM studies at room temperature (and above).[5] In the latter studies, STM images of island distributions were obtained on broad terraces (at least 1000 Å wide). The first image was obtained typically 15–45 min after deposition. Monitoring the subsequent time evolution of the island distribution allowed estimation of the island densities at the time of deposition via a extrapolation of $N_{\rm av}$ back to this time. It is instructive to show in Fig. 1(a) a typical image of an island distribution obtained by deposition of 0.26 ML of Ag on Ag(100). (Note that some restructuring of small overlapping pairs of islands to form a single near-square island is possible since deposition.) It is just this type of island distribution on which the HRLEED studies are performed. Thus, we emphasize again (cf. Sec. I) that the islands are *not* distributed randomly in space. Instead, there is a depletion of nearby pairs of islands, as quantified by the island-island separation distribution shown in Fig. 1(b).

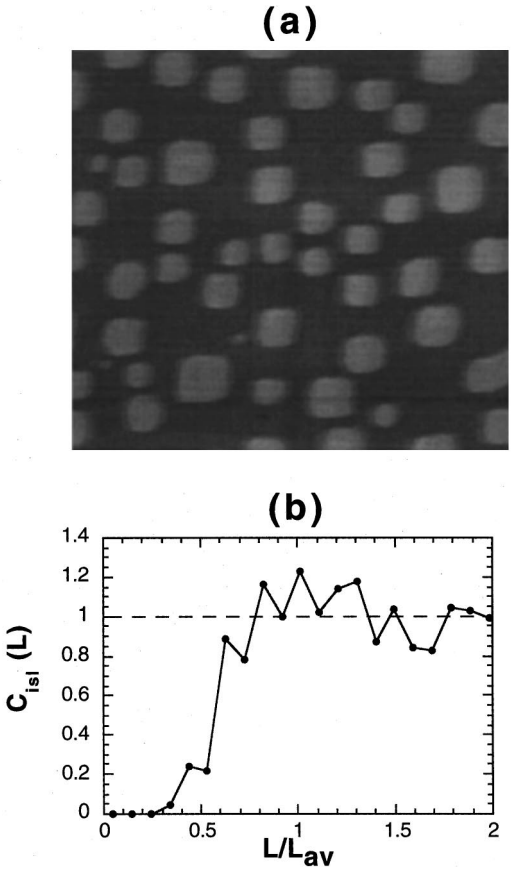

FIG. 1. (a) STM image (110×100 nm^2) of 0.26 ML Ag deposited on Ag(100) at 295 K with $F\approx2\times10^{-3}$ ML/s. Here $N_{\rm av}\approx3.6\times10^{-3}$ nm^{-2}, so $L_{\rm av}\approx17$ nm. (b) The normalized island-island separation distribution, measuring island center-to-center separations L. Despite significant noise in the data due to limited statistics, dramatic depletion is evident for separations $L\lesssim L_{\rm av}/2$.

III. KINEMATIC DIFFRACTION THEORY

Within the kinematic approximation, the diffracted intensity for a lateral momentum transfer **q**, and vertical momentum transfer q_z, is given by[2–4,8]

$$I(\mathbf{q},q_z)\propto(2\pi)^2\{1-2[\theta+\theta^2][1-\cos(q_z b)]\}\delta(\mathbf{q}) + 2[1-\cos(q_z b)]I_{\rm diff}(\mathbf{q}), \quad (1)$$

for **q** near the (0,0) spot and where again b is the interlayer spacing. The first term in the sum is the Bragg δ-function intensity, and the second term is the diffuse intensity. At the in-phase condition, $q_z b=2n\pi$, there is no interference between scattering from different layers, so the diffuse intensity vanishes, and $I\propto(2\pi)^2\delta(\mathbf{q})$ is coverage independent. At the out-of-phase condition, $q_z b=(2n+1)\pi$, interference between different layers is maximum, and thus the diffuse intensity is maximized. The term $I_{\rm diff}(\mathbf{q})=\Sigma_{\mathbf{r}}\exp(i\mathbf{q}\cdot\mathbf{r})C(\mathbf{r})$ corresponds to the diffuse intensity for the overlayer, and is determined by the associated two-point correlation function $C(\mathbf{r})$.[8] (See the Appendix for an alternative formulation.) Due to depletion, this correlation function exhibits a local minimum or ''weak oscillation,'' which produces the *ring* in the diffraction profile upon Fourier transformation.[8] Also, we should emphasize that the experimentally observed intensities actually correspond to the above expression convoluted with an instrument response function, and also modified by the finite terrace widths.[4] Thus, for example, the Bragg in-

TABLE I. L_{av} and $L_c = 4\pi/d^*$ (in units of the surface lattice constant) versus h/F at 0.3 ML; also shown is the effective value of the exponent, p_{eff}, in the relation $L_{av} \sim (h/F)^{p_{eff}}$.

h/F	L_{av}	L_c	$\lambda = L_c/L_{av}$	p_{eff}
10^3	5.2	8.0	1.5	0.129
10^4	7.0	10.7	1.5	0.146
10^5	9.8	15.3	1.6	0.153
10^6	13.9	22	1.6	0.160
10^7	20.2	32	1.6	0.165

tensity is correspondingly broadened, as will be clear in the experimental profiles shown in Sec. IV.

The key quantity extracted directly from experiment is the diameter d^* of the ring in the diffraction intensity, measured from the profile in the $\langle 110 \rangle$ direction. This quantity is typically recast as a real-space correlation length $L_c = 4\pi/d^*$. Usually L_c is identified as the mean island separation $L_{av} = N_{av}^{-1/2}$. However, the precise relationship between L_c and L_{av} is nontrivial (cf. Sec. II), and is determined immediately below.

The required analysis of the kinematic diffraction profile is achieved via Monte Carlo simulations of a canonical model for irreversible nucleation and growth of square islands.[8] The only model parameters are deposition rate F and (total) hop rate for isolated adatoms on terraces, $h = z\nu \exp[-E_d/(k_B T)]$. Here, $z = 4$ is the coordination number for the square lattice of adsorption sites on the fcc(100) surface. In this model, dimers and larger islands are treated as immobile, and islands pairs that ''collide'' due to growth do not restructure, but continue to grow as overlapping squares. The individual constituents of such clusters of partly overlapping islands are counted separately in determining N_{av}. For a fixed coverage of $\theta = 0.3$ ML (corresponding to the experiments), we have determined L_{av} as a function of h/F, and also evaluated the corresponding $I_{diff}(\mathbf{q})$, and thus d^* and L_c. The variation of L_{av} and L_c with h/F is shown in Table I. As expected from classic nucleation theory,[8,9] one finds the scaling $L_{av} \approx 1.37(h/F)^p$ (measured in units of the surface lattice constant), for sufficiently large h/F, with the classic exponent of $p \approx \frac{1}{6}$ for irreversible island formation. The *key observation* is that if one writes $L_c = \lambda L_{av}$, then λ is *not* unity, as commonly assumed, but rather $\lambda \approx 1.6$ for this model at 0.3 ML.

It is appropriate to make some other comments about this key factor λ. First, recall that most island nucleation occurs for low coverages, after which N_{av} and L_{av} are essentially constant, while islands just grow in size. However, the form of the spatial correlation functions changes significantly with coverage, due to island growth, and thus so should λ. In fact, λ increases significantly with coverage up to at least 0.5 ML.[17] Second, note that depletion of nearby island pairs becomes more dramatic with the onset of reversibility in island nucleation.[9,18] This also affects the correlation functions, and thus λ. Finally, we have performed analysis of a modified model incorporating some restructuring of islands upon collision to form a single larger square island.[19] Limited results suggest that the associated increase in L_{av}, relative to the canonical model (due to a decrease in N_{av}, since collided islands are no longer counted separately), is roughly matched by an increase in L_c. Together, these features roughly preserve the value of λ.

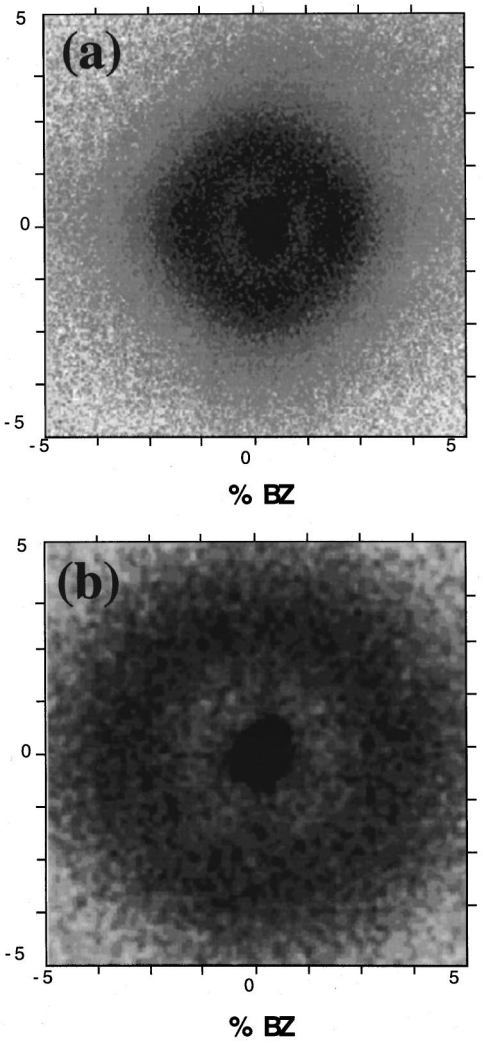

FIG. 2. Gray scale image of variation of the diffracted intensity with lateral momentum transfer, measured as a fraction of the Brillouin-zone (BZ) width, near the (0,0) beam. The intensities were measured following deposition of 0.3 ML of Ag on Ag(100) for (a) $T = 295$ K and $F = 2.4 \times 10^{-3}$ ML/s; (b) $T = 230$ K and $F = 2.0 \times 10^{-3}$ ML/s.

IV. HRLEED RESULTS AND DIFFUSION BARRIER ESTIMATION

Gray scale images of the diffracted intensity as a function of lateral momentum transfer for deposition of 0.3 ML of Ag on Ag(100) at 295 and 230 K are shown in Fig. 2. The features at 295 K are much narrower than at 230 K, reflecting the larger characteristic lengths. However, in both cases, the intensity displays an *inner circular ring*, separated from an *outer feature* revealing weak fourfold symmetry. Similar behavior was observed previously for HRLEED intensities obtained during Cu/Cu(100) homoepitaxy, and a detailed discussion was provided.[12] The inner ring reflects the near circularly symmetric depletion in the island separation distribution, its diameter being controlled by the mean island

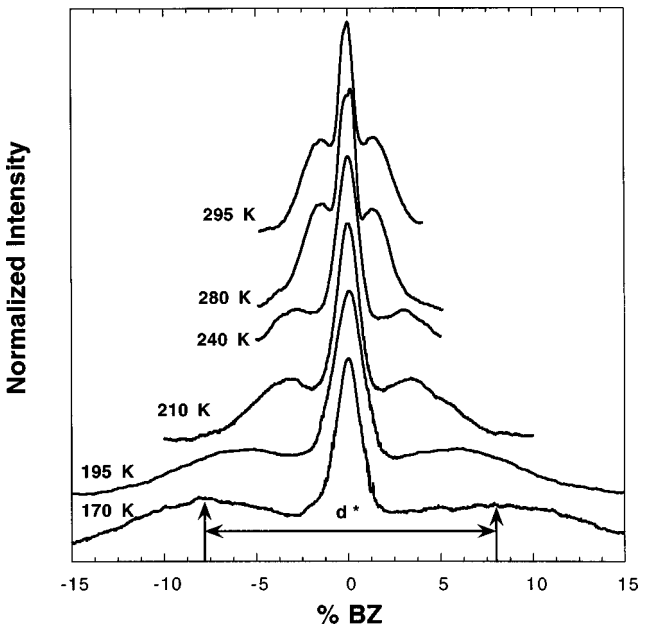

FIG. 3. Temperature dependence of the splitting of the diffraction profiles for 0.3 ML of Ag on Ag(100). Profiles are shown for 295 K (with $F=2.4\times10^{-3}$ ML/s), 280 K (with $F=2\times10^{-3}$ ML/s), 240, 210, 195, and 170 K (with $F=3.7\times10^{-3}$ ML/s). Shown is the logarithm of normalized intensities, where normalization is relative to their maximum values.

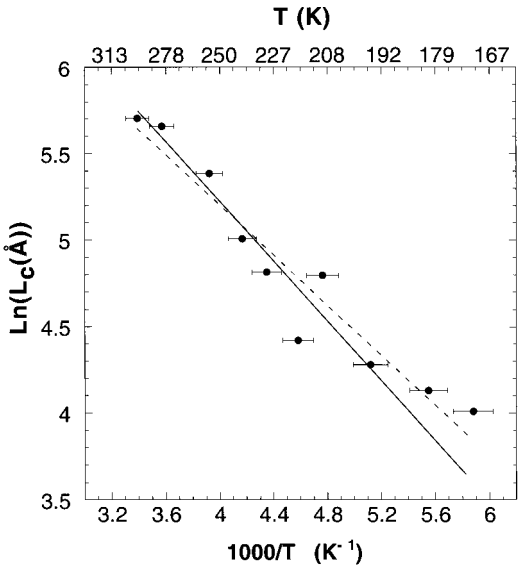

FIG. 4. Arrhenius behavior of the correlation length $L_c=4\pi/d^*$. Data are shown for temperatures and fluxes of (295 K, 2.4×10^{-3} ML/s), (280 K, 2×10^{-3} ML/s), (255 K, 4×10^{-3} ML/s), (240 K, 3.7×10^{-3} ML/s), (230 K, 2×10^{-3} ML/s), (218 K, 2.5×10^{-3} ML/s), (210 K, 3.7×10^{-3} ML/s), (195 K, 3.7×10^{-3} ML/s), (180 K, 3.7×10^{-3} ML/s), and (170 K, 3.7×10^{-3} ML/s). The dashed line is the linear fit to all data producing $E_d\approx0.37$ eV, and the solid line neglects the 180- and 170-K data producing $E_d\approx0.45$ eV.

separation $L_{\rm av}$. The outer feature reflects the shape and size distribution of individual islands, its location being controlled by the smaller mean linear island size $R_{\rm av}=\theta^{1/2}L_{\rm av}=0.55L_{\rm av}$ at 0.3 ML. This outer feature is described well by a ''random-phase approximation'' that neglects interference between scattering from different islands. Its weak fourfold symmetry reflects the near-square shape of individual islands, together with an averaging over the distribution of island sizes. See the Appendix.

Figure 3 summarizes the dependence of the splitting of the diffraction profiles, for 0.3 ML of Ag on Ag(100), on deposition temperature between 170 and 295 K. Fluxes were in the range $F\approx2-4\times10^{-3}$ ML/s. These profiles show the systematic decrease in the ring diameter with increasing temperature. A corresponding Arrhenius plot of $L_c=4\pi/d^*$ is given in Fig. 4. From our previous STM study, it is known that island formation is irreversible at and below room temperature, and that the mobility of dimers and other small clusters is not significant.[5] Then, from nucleation theory,[8,9] it follows that both L_c and $L_{\rm av}$ should scale like $\exp[-pE_d/(k_BT)]$, where $p\approx\frac{1}{6}$ (cf Table I). Using Arrhenius data from the full range 170–295 K, one obtains

$$L_c\approx3.26\times10^3\ \exp[-E_d/(6k_BT)]\ \text{Å}$$

with $E_d\approx0.37\pm0.06$ eV. Instead, using only data from 195–295 K, one obtains

$$L_c\approx5.78\times10^3\ \exp[-E_d/(6k_BT)]\ \text{Å}$$

with $E_d\approx0.45\pm0.06$ eV. The latter choice is prompted by the possibility that classic scaling begins to break down at the lower end of the observed temperature range, as discussed further in Sec. V.

V. DISCUSSION AND COMPARISON WITH STM OBSERVATIONS

Our previous STM study of island density behavior in the Ag/Ag(100) system indicated that $N_{\rm av}\approx(2.3\pm0.2)\times10^{-4}F^{0.31\pm0.02}$ Å^{-2}, for deposition at 295 K.[5] This value of the exponent of 0.31 demonstrates that island formation is irreversible, and that mobility of dimers and other small clusters is not significant during island nucleation. Then, by comparison with results from our model for irreversible nucleation and growth of square islands, we estimate that $h\approx1.6\times10^7$ s^{-1} at 295 K. If one chooses the estimate $E_d=0.37$ eV from Sec. IV using data for the full T range, then one has a prefactor of $\nu\approx10^{13}$ s^{-1}. Simulations with these parameters produce the scaling

$$L_{\rm av}\approx1.86\times10^3\ \exp[-E_d/(6k_BT)]\ \text{Å}$$

for $F=3.7\times10^{-3}$ ML/s, so $\lambda=L_c/L_{\rm av}\approx1.8$. Instead, choosing $E_d=0.45$ eV, using only higher-T data (cf. Sec. IV), yields $\nu\approx1.6\times10^{14}$ s^{-1}, which seems somewhat too high. Simulations with these parameters produce the scaling

$$L_{\rm av}\approx2.98\times10^3\ \exp[-E_d/(6k_BT)]\ \text{Å},$$

for $F=3.7\times10^{-3}$ ML/s, so $\lambda=L_c/L_{\rm av}\approx1.9$. These values of λ appear consistent with the theoretical estimate of $\lambda\approx1.6$ in Sec. III, particularly given the uncertainties in determination of d^* from the experimental data.

Next, we discuss sources of deviation from classic scaling for lower temperatures, and associated refined estimates of E_d. First, it is well known that such deviations occur in canonical models of irreversible nucleation and growth for sufficiently low h/F. See Ref. 8 and Table I. For E_d

$=0.37$ eV and $\nu \approx 10^{13}$ s^{-1}, one still has a large $h/F \approx 10^5$ at 170 K (for $F = 3.7 \times 10^{-3}$ s^{-1}), and simulations predict only a 10% reduction in the scaling exponent and Arrhenius slope from classic values at 170 K. For $E_d = 0.45$ eV and $\nu \approx 10^{14}$ s^{-1}, one has $h/F \approx 10^3$ at 170 K, producing a 30% reduction. Note that at 170 K, for the former choice, one has $L_{\rm av} \approx 10$ lattice constants, and an average island size of $s_{\rm av} = \theta/N_{\rm av} \approx 5 \times 6$ atoms, whereas for the latter one has $L_{\rm av} \approx 6$ lattice constants, and $s_{\rm av} \approx 3 \times 4$ atoms (at 0.3 ML).

The possibility of more extreme ''anomalous'' behavior at lower T was suggested by previous He-atom scattering[11] and HRLEED (Ref. 20) studies of Cu/Cu(100) homoepitaxy. Here, an unexpected plateau in L_c at a high value of ~ 10 lattice constants was observed below 100 K. The plateau was first attributed to significant ''transient mobility'' of isolated deposited atoms.[20] Instead, we believe that it is due to significant restructuring or ''clumping'' of adatoms following deposition. This is possible at such low T only since most atoms are deposited near other adatoms and islands, allowing rearrangement via edge diffusion type processes that have low activation barriers.[21] From Fig. 4, it seems plausible that such a plateau is beginning to emerge in the experimental data for Ag/Ag(100) by 180 K, where island structures are already small (see above). This interpretation is consistent with recent HRLEED experiments by Swan[22] for 0.4 ML of Ag deposited on Ag(100) for a lower temperature range of 110–230 K.

In conclusion, we expect that there is some refinement to classic scaling, primarily due to ''clumping,'' for our lower T range. Accounting for this effect, and the need for a reasonable prefactor, we propose a best estimate of $E_d = 0.40 \pm 0.04$ eV (and $\nu \approx 3 \times 10^{13}$ s^{-1}).

VI. SUMMARY

We have presented results from an HRLEED analysis of island distributions formed by depositing 0.3 ML of Ag on Ag(100) for temperatures between 170 and 295 K. The real-space correlation length L_c, obtained from the splitting of the diffraction profiles, is successfully compared with the average island separation $L_{\rm av}$, based on our previous STM study. However, this requires recognition of a nontrivial relationship $L_c \approx \lambda L_{\rm av}$, with $\lambda \approx 1.6$–1.8 determined by the detailed form of the spatial correlations in the island distribution. Analysis of the temperature dependence of L_c, together with an estimate of the room-temperature mobility from our STM study, leads to an estimate of $E_d = 0.40 \pm 0.04$ eV for the activation barrier for terrace diffusion of Ag on Ag(100), and $\nu \approx 3 \times 10^{13}$ s^{-1} for the prefactor. This should be compared with another experimental estimate of 0.4 eV using low-energy ion scattering, which assessed only the onset of diffusion,[23] and recent estimates from sophisticated *ab initio* electronic structure calculations of 0.52 eV (local-density approximation) and 0.45 eV (generalized gradient approximation),[24] and 0.50 eV (full-potential linear muffin-tin orbital).[25]

ACKNOWLEDGMENTS

This work was supported by NSF Grant No. CHE-9700592. It was performed at Ames Laboratory, which is operated for the U.S. Department of Energy by Iowa State University, under Contract No. 7405-Eng-82.

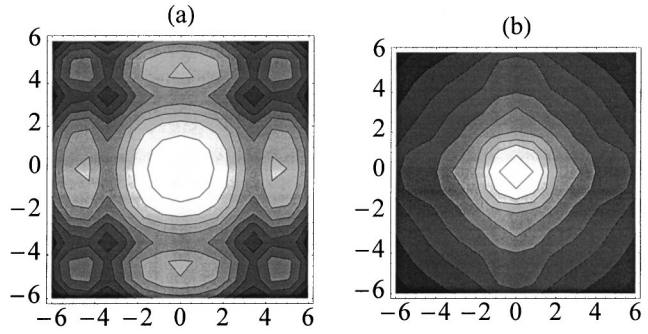

FIG. 5. Gray scale image and contour plot of variation of the logarithm of the diffracted intensity I_0 vs lateral momentum transfer near the (0,0) beam for (a) square islands with a single size; (b) square islands with a realistic distribution of sizes, as determined in Ref. 8. Axes are labeled in units of the momentum transfer multiplied by the average side length of the square islands.

APPENDIX: ISLAND REPRESENTATION FOR THE DIFFUSE INTENSITY

The exact expression in Sec. III for $I_{\rm diff}$ is often recast in an ''island representation'' as a sum $I_{\rm diff} = I_0 + I_{\rm int}$.[2–4] The ''random-phase approximation'' I_0 neglects interference between scattering form different islands, and $I_{\rm int}$ accounts for this interference. Specifically, one has[8]

$$I_0(\mathbf{q}) = \sum_s N_s |\mathcal{A}_s(\mathbf{q})|^2, \quad I_{\rm int}(\mathbf{q}) \approx \left| \sum_s N_s \mathcal{A}_s(\mathbf{q}) \right|^2 \sum_{\mathbf{r}} \exp(i\mathbf{q}\cdot\mathbf{r})[C_{\rm isl}(\mathbf{r}) - 1]. \tag{A1}$$

Here N_s is the density, and $\mathcal{A}_s(\mathbf{q})$ is the average scattering amplitude for islands of size s, and $C_{\rm isl}(\mathbf{r})$ is the island-island correlation function, as in Fig. 1(b). While the expression for $I_{\rm int}$ neglects significant correlations between island size and separation,[26] this formulation provides at least a semiquantitative description of the diffuse intensity. I_0 is obtained by taking the diffracted intensity for a single square island, with edges aligned in the $\langle 110 \rangle$ direction [Fig. 5(a)], and averaging over the appropriate size distribution.[8,26] The result is a monomodal intensity distribution shown in Fig. 5(b), with width reflecting the mean island size. The details are quite sensitive to the form of the size distribution, and are remarkably similar to the experimental plot in Ref. 12. $I_{\rm int}$ has a negative value at $\mathbf{q} = \mathbf{0}$, with a magnitude measuring the ''total amount of depletion'' $\Sigma_{\mathbf{r}}[1 - C_{\rm isl}(\mathbf{r})]$, of nearby island pairs. When combined with I_0, this produces the central ring feature to $I_{\rm diff}$.

*Present address: Département de Physique des Materiaux, Université Claude Bernard, Lyon I, 69622 Villeurbanne, France.

†Present address: Computational Materials Science Department, Sandia National Laboratories, Livermore, CA 94550.

[1] D. P. Woodruff and T. A. Delchar, *Modern Techniques in Surface Science*, 2nd ed. (Cambridge University Press, Cambridge, 1994).

[2] M. A. Van Hove, W. H. Weinberg, and C.-M. Chan, *Low Energy Electron Diffraction* (Springer, Berlin, 1986).

[3] M. Henzler, Appl. Phys. **9**, 11 (1976); Surf. Sci. **73**, 240 (1978); Appl. Surf. Sci. **11**, 450 (1982); Surf. Sci. **132**, 82 (1983); Appl. Phys. A: Solids Surf. **34**, 205 (1984); Surf. Sci. **168**, 744 (1986).

[4] M. G. Lagally, G.-C. Wang, and T.-M. Lu, in *The Chemistry and Physics of Solid Surfaces*, edited by R. Vanselow (CRC, Boca Raton, FL, 1979).

[5] C.-M. Zhang, M. C. Bartelt, J.-M. Wen, C. J. Jenks, J. W. Evans, and P. A. Thiel, J. Cryst. Growth **174**, 851 (1997); Surf. Sci. (to be published); L. Bardotti, M. C. Bartelt, C. J. Jenks, C. R. Stoldt, J.-M. Wen, C.-M. Zhang, P. A. Thiel, and J. W. Evans, Langmuir **14**, 1487 (1998).

[6] J. M. Pimbley and T.-M. Lu, J. Vac. Sci. Technol. A **2**, 457 (1984).

[7] P. Hahn, J. Clabes, and M. Henzler, J. Appl. Phys. **51**, 2079 (1980).

[8] M. C. Bartelt and J. W. Evans, Surf. Sci. **298**, 421 (1993); in *Common Themes and Mechanisms of Epitaxial Growth*, edited by F. Fuoss *et al.*, MRS Symposia Proceedings No. 312 (Materials Research Society, Pittsburgh, 1993), p. 255; Surf. Sci. **284**, L437 (1993). We write $C(\mathbf{r})=P(\mathbf{r})-\theta^2$, where $P(\mathbf{r})$ gives the probability that a pair of sites separated by $\mathbf{r}$ are both occupied. $P(\mathbf{r})$ decreases from a value of roughly θ for small $\mathbf{r}$ (sites are likely either both within or outside an island), to θ^2 for large $\mathbf{r}$ (sites are independently occupied), through a local minimum for $\mathbf{r}$ somewhat larger than the typical island ''radius'' (one site is likely within an island, and the other is in the depletion zone surrounding the island).

[9] J. A. Venables, Philos. Mag. **27**, 697 (1973).

[10] J. A. Stroscio, D. T. Pierce, and R. A. Dragoset, Phys. Rev. Lett. **70**, 3615 (1993); J. A. Stroscio and D. T. Pierce, Phys. Rev. B **49**, 8522 (1994); E. Kopatzki, S. Günther, W. Nichtl-Pecher, and R. J. Behm, Surf. Sci. **284**, 154 (1993); D. K. Flynn-Sanders, J. W. Evans, and P. A. Thiel, *ibid.* **289**, 75 (1993); **298**, 378 (1993).

[11] H.-J. Ernst, F. Fabre, and H. Lapujoulade, Phys. Rev. B **46**, 1929 (1992).

[12] H. Dürr, J. F. Wendelken, and J.-K. Zuo, Surf. Sci. **328**, L527 (1995); J.-K. Zuo, J. F. Wendelken, H. Dürr, and C.-L. Liu, Phys. Rev. Lett. **72**, 3064 (1994).

[13] W. F. Egelhoff and I. Jacob, Phys. Rev. Lett. **62**, 921 (1989); Ch. Ammer, Solid State Phenom. **12**, 73 (1990); Ch. Teichert, Ph.D. thesis, Martin-Luther-Universität Halle-Wittenberg, 1992.

[14] P. Bedrossian, B. Poelsema, G. Rosenfeld, L. C. Jorritsma, N. N. Lipkin, and G. Comsa, Surf. Sci. **334**, 1 (1995).

[15] H. A. van der Vegt, W. J. Huisman, P. B. Howes, and E. Vlieg, Surf. Sci. **330**, 101 (1995).

[16] G. L. Kellogg, Surf. Sci. Rep. **21**, 1 (1994).

[17] J. W. Evans and M. C. Bartelt, in *Morphological Organization in Epitaxial Growth and Removal*, edited by Z. Zhang and M. G. Lagally (World Scientific, Singapore, 1998).

[18] J. W. Evans and M. C. Bartelt, J. Vac. Sci. Technol. A **12**, 1800 (1994).

[19] J. W. Evans and M. C. Bartelt, in *Surface Diffusion: Atomistic and Collective Processes*, edited by M. C. Tringides (Plenum, New York, 1997).

[20] G. L. Nyberg, M. T. Kief, and W. F. Egelhoff, Phys. Rev. B **48**, 14 509 (1993).

[21] ''Transient mobility'' is not observed in molecular dynamic simulations. See, e.g., J. W. Evans, D. E. Sanders, P. A. Thiel, and A. E. DePristo, Phys. Rev. B **41**, 5410 (1990). ''Clumping'' is discussed in more detail by M. C. Bartelt and J. W. Evans, Surf. Sci. (to be published) and by M. Breeman (unpublished).

[22] A. K. Swan (private communication).

[23] M. H. Langelaar, M. Breeman, and D. O. Boerma, Surf. Sci. **352-354**, 597 (1996).

[24] B. D. Yu and M. Scheffler, Phys. Rev. Lett. **77**, 1095 (1996).

[25] G. Boisvert, L. J. Lewis, M. J. Puska, and R. M. Nieminen, Phys. Rev. B **52**, 9078 (1995).

[26] M. C. Bartelt and J. W. Evans, Phys. Rev. B **54**, R17 359 (1996).